International Institute for
Applied Systems Analysis
I I A S A www.iiasa.ac.at

A mathematical model of the stoichiometric control of Smad complex formation in TGF-B signal transducion pathway

Nakabayashi, J. and Sasaki, A.

IIASA Interim Report
June 2009

International Institute for
Applied Systems Analysis
Schlossplatz 1
A-2361 Laxenburg, Austria

Tel: +43 2236 807 342
Fax: +43 2236 71313
E-mail: publications@iiasa.ac.at
Web: www.iiasa.ac.at

Interim Report **IR-09-077**

A mathematical model of the stoichiometric control of Smad complex formation in TGF-B signal transduction pathway

Jun Nakabayashi (nakabayashi_jun@soken.ac.jp)
Akira Sasaki (sasaki_akira@soken.ac.jp)

Approved by

Ulf Dieckmann
Leader, Evolution and Ecology Program

June 2010

Contents

A mathematical model of the stoichiometric control of Smad complex formation in TGF-β signal transduction pathway

Jun Nakabayashi∗# and Akira Sasaki∗ † ‡

∗ Department of Evolutionary Study of Biosystems,
The Graduate University for Advanced Studies (SOKENDAI),
Hayama, Kanagawa 240-0193, Japan
Phone: +81-46-858-1580
Facsimile: +81-46-858-1542
† Evolution and Ecology Program,
International Institute for Applied Systems Analysis,
A-2361 Laxenburg, Austria
‡ PRESTO, Japan Science and Technology Agency,
4-1-8 Honcho Kawaguchi, Saitama, Japan
Corresponding author, email: nakabayashi_jun@soken.ac.jp

April 16, 2009

Abstract

Cell fate in multicellular organism is regulated by the diffusible factor from surrounding cells in concentration-dependent manner. TGF-β is a large protein family of the diffusible proteins secreted from a localized source. The signal of TGF-β is transduced by Smad family transcription factor. Though it is well known that the stoichiometry of Smads in the transcriptional complex regulates the specificity of target genes of TGF-β signal, little is known what the stoichiometry of Smads in the transcriptional complex is determined in TGF-β signal transduction in concentration dependent manner. To investigate the dynamics of Smad complex formation, we construct a two-compartment model for Smad complex formation in TGF-β signal transduction. A simplified one-way oligomerization model, which ignores dissociation and well appropriate the full model under high expression levels of R- and Co-Smad, is constructed to analytically investigate the effect of the oligomerization of Smad. Our one-way model reveals that not only shuttling of the Smad from the cytoplasm to the nucleus but also the preferential accumulation of the heteromeric complex in oligomerization can contribute to the predominant production of the heteromeric complex of Smad including both R- and Co-Smad. It is also shown that oligomerization of Smad can contribute to the specificity of signal transduction. In endothelial cells, both Smad-1/5/8 and -2/3 pathways are activated by TGF-β. The difference of the activity between the two pathways is amplified by trimerization but not by dimerization, suggesting possible importance of trimerization in maintaining the specificity of signal transduction.

Keywords: Smad,signal transduction,transcriptional complex formation, stoichiometry of oligomers

1 Introduction

In multicellular organisms, the behavior of an individual cell is regulated by various signals from the neighboring cells. The members of TGF-β super family are well known diffusible signal molecules or morphogens that regulate cell proliferation and differentiation (Podos & Ferguson, 1999; Gurdon & Bourillot, 2001; Green, 2002). In the developmental process, secreted from a localized source, diffusible TGF-βs determine the fate of the cell receiving them in a concentration-dependent manner. The signal of TGF-β is transduced by Smad family member transcription factors (Massague *et al.*, 2005; Feng & Derynck, 2005; ten Dijke & Hill, 2004; Shi & Massague, 2003; Hill, 2001; ten Dijke *et al.*, 2000; Miyazono, 2000; Kawabata *et al.*, 1999). The TGF-β signal transduction by Smads is the key mechanism interpreting the information of TGF-β ligand. Three critical process, phosphorylation of R-Smad, Smad complex formation, and nuclear import of Smad complex, are thought to control the TGF-β signal transduction.

When cells receive the TGF-β signal, the Smad protein is phosphorylated by the active receptor complex of TGF-β, which initiates the intracellular signal transduction pathway. Phosphorylated Smads form the transcriptional complex with other components and move to the nucleus (Yeo *et al.*, 1999). The transcriptional complex then positively or negatively regulates the expression of specific target genes determining cell fates. In the cytoplasm, there are several kinds of Smad proteins differing in their functions. The transcriptional activity of the target gene is specified by the combination of Smads and cofactors included in the transcriptional complex. *In vitro* experiments revealed that the stoichiometry of Smad complex, the numbers of R- and Co-Smad molecules consisting of a complex, differs widely in transcriptional complexes resulting in their differential binding to specific *cis*-acting elements of gene. For example, two Smad2, one Smad4 and a cofactor FAST-1 consist of a transcriptional complex in activin responsive element of *Xenopus Mix.2* gene promoter. Whereas, one Smad3, one Smad4 and unknown transcription factor consist of a transcriptional complex in SBR of c-jun promoter (Inman & Hill, 2002). Because the transcrip-

tional complex composed of Smads and cofactors plays a critical role in determining the expression of the target genes and cell fates, it is important to understand what combination of Smads and cofactors is formed in the transcriptional complex under given initial concentrations of Smad member monomers and the concentration of signal molecules (e.g. ligand concentration). Though the role of heteromeric complex of Smad (Smad2/2/4 and Smad3/4) in the transcriptional complex is clarified, that of the homomeric complex (Smad2/2 or Smad2/2/2) is elusive. As many kinds of Smad oligomers including homo-dimer, homo-trimer, hetero-dimer and hetero-trimer can be produced in a signal transduction pathway, it is important to understand the conversion efficiency of the heteromeric Smad complex which have the role in target gene regulation.

The kinetic models of Smad signal transduction has been proposed by Schmierer *et al.* who show the importance of the nucleo-cytoplasmic shuttling of Smad for the TGF-β signal transduction(Schmierer *et al.*, 2008). We construct a mathematical model following their model, which is extended to include not only the dimerization but also trimerization of Smad. This model represent the whole process of Smad complex formation in response to TGF-β signal, such as receptor activation by TGF-β ligand, degradation of active receptor, phosphorylation and dephosphorylation of R-Smad, association and dissociation of Smads, and shuttling of Smad from cytoplasm to nucleus. We investigate the dynamics of TGF-β signal transduction via Smad pathway by using this two-compartment model.

We next consider a single-compartment model eliminating the cytoplasm-nucleus structure of cell to clarify the effect of the compartmentalization of cell for Smad complex formation by comparing two-compartment model with single-compartment model. Lastly we consider a simplified one-way oligomerization model that focuses only on oligomerization of Smad (i.e. ignores dissociation). We verified that one-way model well approximate the full two-compartment model under high expression level of R- and Co-Smads monomers. We then analytically study the effect of the oligomerization of Smad for TGF-β signal transduction compared the result with the numerical results of two-compartment model.

2 A model for Smad complex formation

We construct a mathematical model of TGF-β signal pathway following Schmierer's model (Schmierer *et al.*, 2008). We then extend their model by including the trimerization in addition to the dimerization. The chemical reaction equation is summarized in Table1 and a set of the dynamic equations of the full kinetics model are shown in Appendix A. The process of the intracellular signal transduction is schematically shown in Fig 1 and briefly explained below. Cell is partitioned into two compartments, the cytoplasm and the nucleus. R-Smad denoted by R_0 is expressed as an inactive monomer in the absence of the signal. Smad monomers are transported between cytoplasm and nucleus with the import rate constant K_{in} and the export rate constant K_{out} independently of the signal. The localization of Smads are indicated by superscript in Appendix A. Signal transduction starts on the membrane when a TGF-β ligand bind a specific receptor with the association rate constant α to form an active receptor complex. Active receptor is degraded with the degradation rate constant δ_r. Receptor mediated Smad, R-Smad, is phosphorylated by this activated TGF-β receptor with the reaction rate constant γ. Phosphorylated R-Smad then begin to oligomerize.

Smad proteins have two conserved domains, MH-1 and -2, in their amino acid sequences, and between them there is a linker region. An inactive Smad has a bending shape at the linker. Once the C-terminal SxS motif of R-Smad is phosphorylated, R-Smad is stretched and can bind another member of Smad family called common-mediator Smad (Co-Smad) (Moustakas & Heldin, 2002; Wu *et al.*, 2001; Kawabata *et al.*, 1998; ten Dijke & Hill, 2004). Co-Smad lacks the SxS motif in its C-terminus and is not subject to phosphorylation. Phosphorylated R-Smad monomer and Co-Smad monomer are designated by R_1 and C_1, respectively. Phosphorylated R-Smad can associate both with itself and common Smad with the association rate constant μ_i. Because Smad proteins interact with each other through the well conserved amino acid sequence, we assume that association constants, μ_1, μ_2, μ_3, μ_4 and μ_5 are the same. Four kinds of Smad complexes, homomeric and heteromeric dimer or trimer dissociate with the dissociation rate constant λ_i per

binding site. The reaction equation of the Smad oligomerization is briefly summarized as a chemical reaction equation as follows:

$$\begin{aligned}
\mathrm{R}_1 + \mathrm{R}_1 &\underset{\lambda_1}{\overset{\mu_1}{\rightleftarrows}} \mathrm{R}_2 \\
\mathrm{R}_1 + \mathrm{R}_2 &\underset{2\times\lambda_2}{\overset{\mu_2}{\rightleftarrows}} \mathrm{R}_3 \\
\mathrm{R}_1 + \mathrm{C}_1 &\underset{\lambda_3}{\overset{\mu_3}{\rightleftarrows}} \mathrm{C}_2 \\
\mathrm{R}_1 + \mathrm{C}_2 &\underset{\lambda_4}{\overset{\mu_4}{\rightleftarrows}} \mathrm{C}_3 \\
\mathrm{R}_2 + \mathrm{C}_1 &\underset{\lambda_5}{\overset{\mu_5}{\rightleftarrows}} \mathrm{C}_3
\end{aligned} \tag{1}$$

The abbreviations are shown in Table1. The localization of these oligomers is indicated by superscript in Appendix A. Oligomerization of Smad proceeds both in the cytoplasm and the nucleus. Produced Smad oligomers irreversibly move into nucleus with the import rate constant K^*_{in}. Phosphorylated R-Smad monomer are dephosphorylated in the nucleus by phosphatase with the reaction rate constant δ_p. It is assumed that phosphorylated R-Smad is constantly dephosphorylated by the phosphatase. The parameters and the initial concentrations of TGF-β, TGF-β receptor, R-Smad, and Co-Smad used in this model are cited from Schemierer's results. Those are summarized in Table 3. The initial concentrations of TGF-β, inactive TGF-β receptor, and inactive R-Smad monomer and Co-Smad monomer are positive value. Other components are absent in cell before stimuli. The total concentration of R- and Co-Smad monomer are conserved during the signal transduction.

Time course of the Smad phosphorylation and oligomerization both in cytoplasm and nucleus obtained from two-compartment model is shown in Fig 2A to D. The initial concentration of R-Smad in cytoplasm is higher than that of Co-Smad because the export rate of R-Smad to nucleus is higher than that of Co-Smad. Inactive R-Smad is accumulated in cytoplasm before stimuli. The concentration R_0 of inactive R-Smad is decreased by the phosphorylation when the signal transduction starts at time 0. The concentration C_1 of Co-Smad monomer is also decreased by its binding to phosphorylated R-Smad. The concentrations of Smad dimers and trimers in the cytoplasm are then increased as the phosphorylation of R-Smad proceeds. The concentrations of Smad

oligomers in cytoplasm are much lower than those in nucleus because of the irreversible import of Smad oligomers to nucleus. In this case, hetero-dimer is predominantly accumulated in nucleus in response to the signal. In the following we ask which Smad species is predominantly produced in response to the TGF-β signal.

3 Effect of the initial ratio of R-Smad to Co-Smad

We here ask which Smad oligomer is predominantly accumulated in the nucleus in response to the signal. To change the initial ratio of R-Smad to Co-Smad, we varied the initial concentration of R-Smad while that of Co-Smad being kept constant. The peak concentration of the Smad oligomers in the nucleus, the maximum value of R_2^{nuc}, R_3^{nuc}, C_2^{nuc} and C_3^{nuc} during the signal transduction, are plotted as a function of the ratio of the R-Smad to the Co-Smad in Fig 3. The result indicates that hetero-dimer is predominantly accumulated in the nucleus in response to the signal for small to intermediate R-Smad/Co-Smad ratio of the initial monomer concentrations. The result that the heteromeric complex Smad is predominantly produced agree with Schmierer's result even though the trimerization is added in our model. For a large R-Smad/Co-Smad ratio around from 4 to 5, hetero-trimer is predominantly produced. For even larger R-Smad/C-Smad ratio, homomeric dimer and trimer of Smad are predominantly produced. According to Schmiere's data, the ratio of endogenous R-Smad to Co-Smad is smaller than 1. The hetero-dimer is predominantly produced in this R/C ratio.

4 Effect of the compartmentalization of cell for oligomerization of Smad

To clarify the effect of the compartmentalization of cell for Smad complex formation in response to TGF-β signal, a model eliminating the compartment from full kinetics model is constructed. In this single-compartment model, Smads in the nucleus and the cytoplasm are not distinguished.

The oligomerization process is as same as that in the two-compartment model described in (1).

$$
\begin{aligned}
\frac{d[\mathrm{TGF}\beta]}{dt} &= -\alpha_1[\mathrm{TGF}\beta][\mathrm{T}\beta\mathrm{R}] \\
\frac{d[\mathrm{T}\beta\mathrm{R}]}{dt} &= -\alpha_1[\mathrm{TGF}\beta][\mathrm{T}\beta\mathrm{R}] \\
\frac{d[\mathrm{T}\beta\mathrm{R}^*]}{dt} &= \alpha_1[\mathrm{TGF}\beta][\mathrm{T}\beta\mathrm{R}] - \delta_r[\mathrm{T}\beta\mathrm{R}^*] \\
\frac{dR_0}{dt} &= -\gamma R_0[\mathrm{T}\beta\mathrm{R}^*] + \delta_p R_1 \\
\frac{dR_1}{dt} &= \gamma R_0[\mathrm{T}\beta\mathrm{R}^*] \\
&\quad -R_1\left(2\mu_1 R_1 + \mu_2 R_2 + \mu_3 C_1 + \mu_4 C_2\right) + 2\lambda_1 R_2 + 2\times\lambda_2 R_3 + \lambda_3 C_2 + \lambda_4 C_4 \\
&\quad -\delta_p R_1 \\
\frac{dR_2}{dt} &= \mu_1 (R_1)^2 - R_2\left(\mu_2 R_1 + \mu_5 C_1\right) + 2\times\lambda_2 R_3 + \lambda_5 C_3 \\
\frac{dR_3}{dt} &= \mu_2 R_1 R_2 - 2\times\lambda_2 R_3 \\
\frac{dC_1}{dt} &= -C_1\left(\mu_3 R_1 + \mu_5 R_2\right) + \lambda_3 C_2 + \lambda_5 C_3 \\
\frac{dC_2}{dt} &= \mu_3 R_1 C_1 - \mu_4 R_1 C_2 + \lambda_4 C_3 \\
\frac{dC_3}{dt} &= \mu_4 R_1 C_2 + \mu_5 R_2 C_1 - (\lambda_4 + \lambda_5) C_3
\end{aligned}
\tag{2}
$$

Initial conditions and parameters are the same in two-compartment model (7) except for the import and export rate of Smads. The peak concentration of Smad oligomers, R_2, R_3, C_2 and C_3 in the single-compartment model, are plotted in Fig 4 as a function of R/C ratio as well as in the two-compartment model. The result obtained from the single-compartment model shows quite similar result (Compare the result in Fig 3 with that in Fig 4). The heteromeric complex of Smad is predominantly produced for small and intermediate R-Smad/Co-Smad ratio of the initial monomer even in the absence of the compartmentalization of cell. This result indicate that not only compartmentalization of cell but also oligomerization itself contributes to predominant production of the heteromeric complex of Smad. The switching R/C ratio from hetero-trimer to homo-trimer obtained from single-compartment model slightly shifts to left as compared with the result obtained from the two-compartment model shown in Fig 3. R/C ratio maximizing the peak concentration of hetero-trimer is around from 3 to 4 in single compartment model (from 5 to 6 in

two-compartment model). This result indicate that the compartmentalization of cell enhances the predominant production of heteromeric complex of Smad in response to the signal.

The import and the export between cytoplasm and nucleus of Smad affect the predominant oligomer species of Smad for a given initial R/C ratio. As shown in Fig 5-A, the peak concentrations of all Smad species monotonically deceases depending on the import rate of R-Smad to nucleus. This is because the concentration of R-Smad is decreased by the accumulation of R-Smad in nucleus because R-Smad is only phosphorylated in cytoplasm by the activated TGF-β receptor. This result indicate that the accumulation of R-Smad in nucleus inhibit the Smad complex formation. On the other hands, the peak concentrations of heteromeric complex of Smad but not homomeric complex of Smad is increased depending on the import rate of Co-Smad as shown in Fig 5-B. The accumulation of Co-Smad does not inhibit the complex formation. The accumulation of Co-Smad specifically enhances the production of the heteromeric complex of Smad.

It is revealed both from the two-compartment and single-compartment model that which Smad oligomer is predominantly produced is primarily determined by the ratio of the initial concentration of R-Smad monomer to that of Co-Smad monomer. Unless the R/C ratio becomes sufficiently large, heteromeric complex of Smad is predominantly produced. This predominancy of heteromeric complex of Smad is caused not only by the compartmentalization of cell but also by preferential accumulation of a specific Smad polymer in oligomerization process.

We also numerically examined the relative peak concentration in two-compartment model over a wide range of parameters, and found that the relative peak concentrations of Smad oligomers are hardly affected by changing the degradation rate of TGF-β receptor, δ_r, or the dephosphorylation rate of R-Smad, δ_p (data not shown). The degradation of active receptor and dephosphorylation of R-Smad contribute to the restoration of Smad to normal condition in a longer time span than oligomerization process (Fig 2, but does not contribute preferential accumulation of heteromeric or homomeric complex of Smad. To summarize the results mentioned above, compartmentalization

of cell, degradation of active receptor and dephosphorylation of R-Smad does not critically affect which Smad species is predominantly produced for given initial R/C ratio.

5 One-way Oligomerization Model

5.1 Effect of the expression level of Smad complex

Un like degradation of TGF-β receptor, dephosphorylation of R-Smad, and compartmentalization of cell, we found, by numerically examining the two-compartment model, that the dissociation of Smad complex and the expression level of Smads do affect the peak concentrations and peak positions of Smad oligomers among the processes of the TGF-β signal transduction. We examine the relative peak concentrations of Smad oligomers in two-compartment model when the expression of Smads is increased. As shown in Fig 6-A, the relative peak concentrations of both homo- and hetero-trimer increase, but the peak concentrations of both homo- and hetero-dimer decrease when the expression of R- and Co-Smad are large as compared with Fig 3. This result indicates that the conversion efficiency of Smad complex formation from monomer to trimer is improved by a larger expression level of R- and Co-Smad. The effect of the dissociation of Smad complex becomes relatively weak as compared with the association of R- and Co-Smad as the expression of Smad increases. This is because the association process has the speed proportional to the product of the concentrations of R- and Co-Smad, while the dissociation has the speed proportional to the concentration of single Smad species. Thus increasing the concentration of Smad promotes the association and demotes the dissociation. We confirm that the improvement of the conversion efficiency of Smad complex formation is achieved in a quite similar way when the dissociation Smad complex is eliminated from the single-compartment model. As shown in Fig 6-B, the peak concentrations of both homo- and hetero-trimer increase when the dissociation rate constant λ is 0 in single-compartment model as well as shown in Fig 6-A. Homomeric complex of Smad is predominantly produced after R/C ratio becomes sufficiently large if dissociation is neglected or the expression level is high. The thresholds R/C ratio at which the predominant Smad species

switches from homo-dimer and hetero-trimer and from hetero-trimer to homo-trimer are similar, but the transitions are much clearer when $\lambda = 0$ or when expression level is large. According to these results, we construct a simplified one-way oligomerization model to investigate the switching mechanism of the preferential production of Smad complex species as a function of R/C ratio. This model well approximate the process of Smad complex formation when the expression level of R- and Co-Smad is sufficiently large.

5.2 One-way oligomerization model

Phosphorylated R-Smad monomer denoted by R_1 can bind either R-Smad monomer (R_1) or Co-Smad monomer (C_1) to form homo-dimer (R_2) or hetero-dimer (C_2). R-Smad homo-dimer can bind either R- or Co-Smad monomer, while RC hetero-dimer can bind only R-Smad monomer. Produced trimers (R_3 and C_3). The concentrations of phosphorylated R-Smad monomer, homo-dimer, homo-trimer, hetero-dimer and hetero-trimer are designated by x_1, x_2, x_3, y_1, y_2 and y_3, respectively. The time change for the concentrations of Smads are

$$\begin{aligned}
\frac{dx_1}{dt} &= -\mu x_1(2x_1 + x_2 + y_1 + y_2) \\
\frac{dx_2}{dt} &= \mu x_1^2 - \mu x_2(x_1 + y_1) - \mu x_2 \\
\frac{dx_3}{dt} &= \mu x_1 x_2 \\
\frac{dy_1}{dt} &= -\mu y_1(x_1 + x_2) \\
\frac{dy_2}{dt} &= \mu x_1 y_1 - \mu y_2 x_1 \\
\frac{dy_3}{dt} &= \mu x_1 y_2 + \mu x_2 y_1
\end{aligned} \tag{3}$$

Here we analyze a generalized model of homo-oligomer and hetero-oligomer in which the final product is composed of n molecules. The homo-oligomer of i R-Smad monomers can bind both homo- and hetero-oligomer composed of j monomers, only when $i + j$ is less than n. Whereas, the hetero-oligomer composed of a single Co-Smad monomer and $j - 1$ R-Smad monomers can bind a

homo-oligomer with i R-Smad monomers (again $i+j \leq n$). The reaction equation is

$$\begin{aligned} \mathrm{R}_i + \mathrm{R}_j &\xrightarrow{\mu} \mathrm{R}_{i+j} \\ \mathrm{R}_i + \mathrm{C}_j &\xrightarrow{\mu} \mathrm{C}_{i+j} \end{aligned}$$

We denote by x_i the concentration of homo-oligomer composed of i molecules of R-Smad, and by y_i the concentration of hetero-oligomer composed of one Co-Smad molecule and $i-1$ R-Smad molecules. The final product of Smad complex is trimer ($n = 3$). The concentrations of the homo-oligomer composed of i R-Smads and the hetero-oligomer composed of a Co-Smad and $i-1$ R-Smads is designated by x_i and y_i, respectively. The time change of the concentrations of Smad oligomers are

$$\begin{aligned} \frac{dx_1}{dt} &= -\mu x_1 \sum_{i=2}^{n-1}((1+\delta_{ij})x_i + y_i) \\ \frac{dx_i}{dt} &= \mu \sum_{k=1}^{[i/2]} x_k x_{i-k} - \mu x_i \sum_{j=1}^{n-i}((1+\delta_{ij})x_j + y_j), \qquad (i = 2, 3, \cdots, n-1), \\ \frac{dx_n}{dt} &= \mu \sum_{i=1}^{[n/2]} x_i x_{n-i} \\ \frac{dy_1}{dt} &= -\mu y_1 \sum_{i=1}^{n-1} x_i \\ \frac{dy_i}{dt} &= \mu \sum_{k=1}^{i-1} x_k y_{i-k} - \mu y_i \sum_{j=1}^{n-i} x_j, \qquad (i = 2, 3, \cdots, n-1), \\ \frac{dy_n}{dt} &= \mu \sum_{i=1}^{n-1} x_i y_{n-i} \end{aligned} \tag{4}$$

Here, $[n/2]$ denotes the largest integer which is less than or equal to $n/2$, and $\delta_{ij} = 1$ if $i = j$ and $\delta_{ij} = 0$ if $i \neq j$. The initial concentration of R- and Co-Smad monomer is designated by $x_1(0) = x_0$, $y_1(0) = y_0$. Whereas, $x_i(0) = y_i(0) = 0$ for $i = 2, 3, \cdots, n$. To simplify the analysis, we non-dimensionalize the above equations by rescaling the concentration $x_i(t)$ and $y_i(t)$ relative to the initial concentration of the total Smad monomers $x_0 + y_0$ as $X_i(t) = x_i(t)/(x_0 + y_0)$ and

$Y_i(t) = y_i(t)/(x_0 + y_0)$ and by rescaling time as $\tau = \mu(x_0 + y_0)t$. This yields

$$\begin{aligned}
\frac{dX_1}{d\tau} &= -X_1 \sum_{i=1}^{n-1}((1+\delta_{ij})X_i + Y_i) \\
\frac{dX_i}{d\tau} &= \sum_{k=1}^{[i/2]} X_k X_{i-k} - X_i \sum_{j=1}^{n-i}((1+\delta_{ij})X_j + Y_j), \qquad (i = 2, 3, \cdots, n-1), \\
\frac{dX_n}{d\tau} &= \sum_{i=1}^{[n/2]} X_i X_{n-i} \\
\frac{dY_1}{d\tau} &= -Y_1 \sum_{i=1}^{n-1} X_i \\
\frac{dY_i}{d\tau} &= \sum_{k=1}^{i-1} X_k Y_{i-k} - Y_i \sum_{j=1}^{n-i} X_j, \qquad (i = 2, 3, \cdots, n-1), \\
\frac{Y_n}{d\tau} &= \sum_{i=1}^{n-1} X_i Y_{n-i}
\end{aligned} \tag{5}$$

The initial conditions are given by $X_1(0) = x_0/(x_0 + y_0)$, $Y_1(0) = y_0/(x_0 + y_0) = 1 - X_1(0)$ and $X_i(0) = Y_i(0) = 0$ for $i = 2, 3, \cdots, n$. This rescaled system (5) has only one parameter, the initial ratio $x(0)/y(0)$ of R-Smad to Co-Smad (R/C ratio), which determines the concentrations of Smad homo-dimers, homo-trimers, hetero-dimer, hetero-trimers and so forth, produced in the cell receiving TGF-β signal.

5.3 Equilibrium concentration of Smad complexes

When enough time has passed since the receipt of TGF-β signal in the cell, all reactions described in (5) stop because all the phosphorylated R-Smad monomers are consumed to form either homo- or hetero-oligomers of Smads. As shown in Fig 7, the equilibrium concentration is determined by the initial ratio of phosphorylated R-Smad to that of Co-Smad. When the initial concentration of phosphorylated R-Smad is smaller than that of Co-Smad, surplus Co-Smads remain as monomers and the hetero-dimer is produced predominantly. This result is independent of number of molecules included in the final product. Heteromeric dimer, trimer, and larger heteromeric complexes are sequentially become predominant as the ratio of the initial concentration of phosphorylated R-Smad to that of Co-Smad increases. When the ratio of initial concentration of R-Smad to that of

Co-Smad, x_0/y_0, is around 2, the production of the hetero-trimer, RRC, is maximized. If the ratio is further increased, homo-oligomer composed of n molecules of R-Smad becomes predominant in the final product.

5.4 phosphorylation speed of R-Smad

We relax the condition that all R-Smad is phosphorylated when the signal transduction has started. The phosphorylation of R-Smad is described

$$\text{R-Smad} \quad \stackrel{\hat{\gamma}}{\rightarrow} \quad \text{phosphorylated R-Smad},$$

In active R-Smad is constantly phosphorylated. The concentration of active receptor complex is constant. The concentration of inactive R-Smad is designated by x_0. The time change of inactive and phosphorylated R-Smad is then

$$\begin{aligned} \frac{dx_0}{dt} &= -\hat{\gamma}x_0 \\ \frac{dx_1}{dt} &= \hat{\gamma}x_0 - \mu x_1(2x_1 + x_2 + y_1 + y_2). \end{aligned} \tag{6}$$

The concentration x_1 of phosphorylated R-Smads increases by $\hat{\gamma}x_0$ in a unit time interval (see (3) derived later). By this modification, we can see how the process is changed when R-Smad phosphorylation proceeds more slowly. The equilibrium concentration with gradual R-Smad phosphorylation is shown in Fig 7. The result obtained from one-way oligomerization model in Fig 7 is well correspond to that both from two-compartment model with large Smad expression and from single-compartment model without dissociation in Fig 6-A and -B. The switching between the production of hetero-dimer, hetero-trimer and homo-trimer as x_0/y_0 varies becomes much clearer than in Fig 6-A and -B. The concentration of homo-dimer is almost 0 around the all region. The switching mechanism of predominant products is show by (A6) to (A7c) when $r < 2$ and (A10b) to (A12b) when $r > 2$ in Appendix. In addition, the equilibrium concentration of homo-dimer remain small for all values of x_0/y_0. Slow phosphorylation of R-Smad makes the phosphorylated R-Smad monomers supplied gradually, which converts homo-dimer to homo-trimer efficiently.

6 Clear switching by using trimers rather than dimers

The result obtained from the basic oligomerization model analytically reveal that the oligomerization itself plays important role in predominantly producing the heteromeric complex of Smad that regulates the target gene expression in response to TGF-β signal. Next, we investigate what difference between dimerization and trimerization. Especially, the function of oligomerization for specificity of the signal transduction is focused. We apply our simplified model to explain the switching mechanism for the expression of Smad1 and Smad2 in response to the relative concentrations of ALK-1 and ALK-5 signals reached to the endothelium cell. This result indicate that trimerization affect distinguishing the signal under the mixed ligand.

ALK-1 and ALK-5 are known to be simultaneously expressed in endothelial cells as TGF-β receptor(Goumans *et al.*, 2003; Goumans *et al.*, 2002). ALK-1 and -5 have conflicting effect for each other. ALK-1 can phosphorylate Smad-1/5 as R-Smad and activate Smad-1/5 pathway that introduce cell proliferation and migration. On the other hand, ALK-5 can phosphorylate Smad-2/3 as R-Smad and activate Smad-2/3 pathway that repress cell proliferation and migration. The balance between the activity of Smad-1/5 pathway and that of Smad-2/3 pathway determine the cell fate of endothelium. It is reported that the amount of ALK-5 mRNA is higher than that of ALK-1 in bovine aortic endothelium. Inversely ALK-1 is higher in bovine corneal endothelium. The response of endothelium for TGF-β signal is different depending on the ratio of expression level of ALK-5 to that of ALK-1.

We consider the effect of Smad complex formation on the degrees of activation of two alternative signal transduction pathways in endothelium. Our basic oligomerization model is extended to include two R-Smads. Smad-1/5 (i.e., Smad-1 or Samd-5) and Smad-2/3 are designated by R_1 and R_2, respectively. The rule of oligomerization is the same as the previous model. That is, R-Smad can interact with both R-Smad and Co-Smad. Co-Smad can interact only with R-Smads.

The reaction equation of dimerization is

$$\begin{aligned} \mathrm{R}_i + \mathrm{R}_j &\rightarrow \mathrm{R}_i\mathrm{R}_j, \qquad (i,j=1,2), \\ \mathrm{R}_i + \mathrm{C} &\rightarrow \mathrm{R}_i\mathrm{C}, \qquad (i=1,2). \end{aligned}$$

Three dimer composed of only R-Smads (R_1R_1, R_1R_2, R_2R_2) can interact with two R-Smads and Co-Smads further to form trimer. While two hetero dimers (R_1C, R_2C) can interact with two R-Smads. As a result, 7 kinds of trimers ($R_1R_1R_1$, $R_1R_1R_2$, $R_1R_2R_2$, $R_2R_2R_2$, R_1R_1C, R_1R_2C, R_2R_2C) are produced by this complex formation. the chemical reaction equations for trimerization are

$$\begin{aligned} \mathrm{R}_i\mathrm{R}_j + \mathrm{R}_j &\rightarrow \mathrm{R}_i\mathrm{R}_j\mathrm{R}_k, \qquad (i,j,k=1,2), \\ \mathrm{R}_i\mathrm{R}_j + \mathrm{C} &\rightarrow \mathrm{R}_i\mathrm{R}_j\mathrm{C}, \qquad (i,j=1,2), \\ \mathrm{R}_i\mathrm{C} + \mathrm{R}_j &\rightarrow \mathrm{R}_i\mathrm{R}_j\mathrm{C}, \qquad (i,j=1,2). \end{aligned}$$

The trimer composed of two R_1s and one C is final product of the signal transduction introduced by ALK-1. While R_2R_2C is the final product of the signal transduction introduced by ALK-5. To compare the equilibrium concentration of these two trimers, activity ratio of ALK-1 to ALK-5 signal transduction are investigated.

The time change of each concentration are given by the law of mass action. The equilibrium concentration is obtained as the concentrations after sufficiently long time has passed. It is assumed that the initial concentration of R_1 and R_2 are proportional to the expression level of ALK-1 and -5, respectively.

The ratio of the equilibrium concentration of R_1R_1C (the signal transducer of ALK-1) to that of R_2R_2C (the signal transducer of ALK-5) is plotted against the ratio of the initial concentration of R_1 to that of R_2 in Fig 8, in logarithmic scales in both axes. Dashed line show the same results when the final products are hetero-dimers rather than hetero-trimers. Comparison of these two curves shows that the switching between a hetero-trimer and another hetro-trimer by changing

the initial R-Smads concentration is much sharper than than the switching between hetero-dimers.

7 Discussion

We construct a mathematical model of the TGF-β signal transduction following the Schmierer's model and extended it by including the trimerization of Smad. Even when trimerization is taken into consideration, the Schmiere's compartmentalized model explain the predominant production of the heteromeric complex of Smad. We however found the qualitatively quite similar results by using the single-compartment model for what Smad species is predominantly produced as a function of the ratio of the initial concentration of R-Smad to that of Co-Smad. To understand what determines the predominant Smad species, we compare the results of compartmentalized model with that of single-compartment model (2) and the further simplified one-way oligomerization model (5). Tough the conversion efficiency from Smad monomer to trimer increases in the one-way oligomerization model (5), the relationship between predominant Smad species produced in response to the signal and R/C ratio is qualitatively conserved. We investigate the equilibrium concentration of Smad oligomers in one-way oligomerization model. The equilibrium concentrations of Smad oligomers are determined by the ratio of R/C ratio. When R/C ratio is low, the hetero-dimer is predominantly produced. The predominant produced heteromeric complex shifts from the hetro-dimer to hetero-trimer as R/C ratio increases. It is reported that Smad homo-oligomer cannot be detected when Smad4, which is Co-Smad, is expressed excessively (Kawabata *et al.*, 1999), as is compatible with our result. It is reported that the hetero-oligomer of Smad can contribute to regulate the target gene expression in response to the TGF-β signal. On the other hand, the function of homomeric complex of Smad is not clear yet. The predominant production of the heteromeric complex of Smad that regulate the target gene expression is reasonable for the TGF-β signal transduction. Our model reveals that not only the compartmentalization of cell but also preferential accumulation of Smad in oligomerization process promotes the predominant production of the heteromeric complex of Smad, especially when R/C ratio is small. Our one-way oligomerization model is very useful

to analytically understand which oligomer is predominantly produced depending on R/C ratio. Especially, the result obtained from two-compartment model well correspond to that from one-way oligomerization model as the expression level of R- and Co-Smad increases.

Next we consider the phosphorylation speed of R-Smad. The speed of phosphorylation is determined by the concentration of active TGF-β receptor complex, R, and association constant between R-Smad and TGF-β receptor, β. The slow phosphorylation decrease the intermediate homo- and hetero-dimer when the initial concentration of R-Smad is larger than that of Co-Smad. Slow phosphorylation ensures a larger parsistence of active R-Smad monomer which can bind both monomer and dimer. Though the hetero- and homo-trimer are increased by the slow phosphorylation, it takes more time to accumulate the final product. Within a finite time scale, an intermediate phosphorylation speed of R-Smad is can maximize the concentration of homo- and hetero-trimer. The conversion efficiency of the protein complex formation is discussed in (Nakabayashi & Sasaki, 2006) in the same context.

We investigate the effect of import rate of R- and Co-Smad, Kr_{in} and Kc_{in}, for the Smad oligomerization in response to the signal. Our two-compartment model reveals that the effect of the import rate of R-Smad to nucleus is different from that of Co-Smad. The initial R/C ratio maximizing the hetero-trimer in the nucleus increases as Kr_{in} increases as shown in Fig 5-A. Conversely, the R/C ratio maximizing the hetero-trimer in the nucleus decreases as Kc_{in} increases as shown in Fig 5-B. When R-Smad monomer is accumulated in the nucleus with a high import rate of R-Smad, the accumulation of Smad oligomers including the R-Smad is enhanced, but the total amount of phosphorylated R-Smad produced during the signal transduction decreases because R-Smad is phosphorylated in the cytoplasm but not the nucleus. As a result, the production of the Smad oligomers is suppressed as the import rate of R-Smad to nucleus increases. On the other hand, the Co-Smad in the nucleus can associate with R-Smad as well as in the cytoplasm. The accumulation of Co-Smad in the nucleus with high import rate does not influences the oligomerization of Smad. The relatively higher import rate of Co-Smad than R-Smad is advantageous for

the predominant production of heteromeric complex of Smad. Under this condition, it is necessary to express more R-Smad to produce the homomeric complex of Smad.

Next, we also examine the advantage of trimerization over dimerization in switching gene expression with two TGF-β receptor. We apply the one-way oligomerization model for the mixed receptor complex in endothelial cells. ALK-1 and ALK-5 are simultaneously expressed in endothelial cells as type I receptor (Goumans *et al.*, 2002; Goumans *et al.*, 2003). ALK-1 and -5 activate Smad-1/5/8 and Smad-2/3, respectively. We expand the model to include two R-Smads. The relative activity is evaluated by the ratio of equilibrium concentration of the trimer composed of two Smad-1/5/8 molecules and one Smad-4 (R_1R_1C) to that of the trimer composed of two Smad-2/3 molecules and one Smad-4 (R_2R_2C). When the final product is trimer, the ratio of the initial concentration of Smad-1 to that of Smad-2 is significantly amplified in the final products. When the final product is dimer the amplification of the ratio of initial concentration of Smad-1 to that of Smad-2 becomes smaller than 1, indicating that the ratio in the final products is decelerated from that of the initial monomer concentrations.

The specific interactions between TGF-β ligand and type II receptor, type II and type I receptor, type I receptor and R-Smad are designed for the specificity of signal transduction. ALK-1$\rightarrow$Smad-1/5 signal transduction pathway has the conflicting effect against ALK-5 $\rightarrow$ Smad-2/3 signal transduction pathway (Byfield & Roberts, 2004). Cells receive mixed signal, but must determine their fate uniquely. Though either ALK-1 or ALK-5 is expressed in many cells, the stoichiometry of ALKs in the ligand receptor complex determine the final activity of TGF-β signal in endothelial cells. Our model reveals that the small difference between ALK-1 and -5 in the active receptor complex is amplified by trimerization but not by dimerization of Smads. The trimeric complex of Smad is useful for the clear switching of the mixed signal. This clear switching is caused by the competition between Smad-1/3/8 and Smad-2/3 over the Co-Smad, but not explicit inhibition each other.

Appendix A

two-compartment model of TGF-β signal transduction is described as follows:

7.1 TGF-β receptor activation and degradation

$$\begin{aligned}
\frac{d[TGF\beta]}{dt} &= -\alpha[TGF\beta][T\beta R] \\
\frac{d[T\beta R]}{dt} &= -\alpha[TGF\beta][T\beta R] \\
\frac{d[T\beta R^*]}{dt} &= \alpha[TGF\beta][T\beta R] - \delta_r[T\beta R^*]
\end{aligned}$$

7.2 Cytoplasmic compartment

$$\begin{aligned}
\frac{dR_0^{\mathrm{cyt}}}{dt} &= -\gamma[T\beta R^*]R_0^{\mathrm{cyt}} - Kr_{\mathrm{in}}R_0^{\mathrm{cyt}} + Kr_{\mathrm{out}}R_0^{\mathrm{nuc}} \\
\frac{dR_1^{\mathrm{cyt}}}{dt} &= \gamma[T\beta R^*]R_0^{\mathrm{cyt}} - Kr_{\mathrm{in}}R_1^{\mathrm{cyt}} + Kr_{\mathrm{out}}R_1^{\mathrm{nuc}} \\
&\quad -R_1^{\mathrm{cyt}}\left(2\mu_1 R_1^{\mathrm{cyt}} + \mu_2 R_2^{\mathrm{cyt}} + \mu_3 C_1^{\mathrm{cyt}} + \mu_4 C_2^{\mathrm{cyt}}\right) \\
&\quad +2\lambda_1 R_2^{\mathrm{cyt}} + 2\lambda_2 R_3^{\mathrm{cyt}} + \lambda_3 C_2^{\mathrm{cyt}} + \lambda_4 C_3^{\mathrm{cyt}} \\
\frac{dR_2^{\mathrm{cyt}}}{dt} &= -Kr_{\mathrm{in}}^* R_2^{\mathrm{cyt}} + \mu_1\left(R_1^{\mathrm{cyt}}\right)^2 - \lambda_1 R_2^{\mathrm{cyt}} \\
&\quad -R_2^{\mathrm{cyt}}\left(\mu_2 R_1^{\mathrm{cyt}} + \mu_5 C_1^{\mathrm{cyt}}\right) + 2\lambda_2 R_3^{\mathrm{cyt}} + \lambda_5 C_3^{\mathrm{cyt}} \\
\frac{dR_3^{\mathrm{cyt}}}{dt} &= -Kr_{\mathrm{in}}^* R_3^{\mathrm{cyt}} + \mu_2 R_1^{\mathrm{cyt}} R_2^{\mathrm{cyt}} - 2\lambda_2 R_3^{\mathrm{cyt}} \\
\frac{dC_1^{\mathrm{cyt}}}{dt} &= -Kc_{\mathrm{in}}C_1^{\mathrm{cyt}} + Kc_{\mathrm{out}}C_1^{\mathrm{nuc}} \\
&\quad -C_1^{\mathrm{cyt}}\left(\mu_3 R_1^{\mathrm{cyt}} + \mu_5 R_2^{\mathrm{cyt}}\right) + \lambda_3 C_2^{\mathrm{cyt}} + \lambda_5 C_3^{\mathrm{cyt}} \\
\frac{C_2^{\mathrm{cyt}}}{dt} &= -Kc_{\mathrm{in}}^* C_2^{\mathrm{cyt}} + \mu_3 R_1^{\mathrm{cyt}} C_1^{\mathrm{cyt}} - \lambda_3 C_2^{\mathrm{cyt}} \\
&\quad -\mu_4 R_1^{\mathrm{cyt}} C_2^{\mathrm{cyt}} + \lambda_4 C_3^{\mathrm{cyt}} \\
\frac{dC_3^{\mathrm{cyt}}}{dt} &= -Kc_{\mathrm{in}}^* C_3^{\mathrm{cyt}} + \mu_4 R_1^{\mathrm{cyt}} C_2^{\mathrm{cyt}} - \lambda_4 C_3^{\mathrm{cyt}} + \mu_5 R_2^{\mathrm{cyt}} C_1^{\mathrm{cyt}} - \lambda_5 C_3^{\mathrm{cyt}}
\end{aligned}$$

7.3 Nuclear compartment

$$
\begin{aligned}
\frac{dR_0^{\mathrm{nuc}}}{dt} &= Kr_{\mathrm{in}}R_0^{\mathrm{cyt}} - Kr_{\mathrm{out}}R_0^{\mathrm{nuc}} + \delta_p R_1^{\mathrm{nuc}} \\
\frac{dR_1^{\mathrm{nuc}}}{dt} &= Kr_{\mathrm{in}}R_1^{\mathrm{cyt}} - Kr_{\mathrm{out}}R_1^{\mathrm{nuc}} - \delta_p R_1^{\mathrm{nuc}} \\
&\quad -R_1^{\mathrm{nuc}}\left(2\mu_1 R_1^{\mathrm{nuc}} + \mu_2 R_2^{\mathrm{nuc}} + \mu_3 C_1^{\mathrm{nuc}} + \mu_4 C_2^{\mathrm{nuc}}\right) \\
&\quad +2\lambda_1 R_2^{\mathrm{nuc}} + 2\lambda_2 R_3^{\mathrm{nuc}} + \lambda_3 C_2^{\mathrm{nuc}} + \lambda_4 C_3^{\mathrm{nuc}} \\
\frac{dR_2^{\mathrm{nuc}}}{dt} &= Kr^*_{\mathrm{in}}R_2^{\mathrm{cyt}} + \mu_1\left(R_1^{\mathrm{nuc}}\right)^2 - \lambda_1 R_2^{\mathrm{nuc}} \\
&\quad -R_2^{\mathrm{nuc}}\left(\mu_2 R_1^{\mathrm{nuc}} + \mu_5 C_1^{\mathrm{nuc}}\right) + 2\lambda_2 R_3^{\mathrm{nuc}} + \lambda_5 C_3^{\mathrm{nuc}} \\
\frac{dR_3^{\mathrm{nuc}}}{dt} &= Kr^*_{\mathrm{in}}R_3^{\mathrm{nuc}} + \mu_2 R_1^{\mathrm{nuc}} R_2^{\mathrm{nuc}} - 2\lambda_2 R_3^{\mathrm{nuc}} \\
\frac{dC_1^{\mathrm{nuc}}}{dt} &= Kc_{\mathrm{in}}C_1^{\mathrm{cyt}} - Kc_{\mathrm{out}}C_1^{\mathrm{nuc}} \\
&\quad -C_1^{\mathrm{nuc}}\left(\mu_3 R_1^{\mathrm{nuc}} + \mu_5 R_2^{\mathrm{nuc}}\right) + \lambda_3 C_2^{\mathrm{nuc}} + \lambda_5 C_3^{\mathrm{nuc}} \\
\frac{C_2^{\mathrm{nuc}}}{dt} &= K^*_{\mathrm{in}}C_2^{\mathrm{cyt}} + \mu_3 R_1^{\mathrm{nuc}} C_1^{\mathrm{nuc}} - \lambda_3 C_2^{\mathrm{nuc}} \\
&\quad -\mu_4 R_1^{\mathrm{nuc}} C_2^{\mathrm{nuc}} + \lambda_4 C_3^{\mathrm{nuc}} \\
\frac{dC_3^{\mathrm{nuc}}}{dt} &= Kc^*_{\mathrm{in}}C_3^{\mathrm{cyt}} + \mu_4 R_1^{\mathrm{nuc}} C_2^{\mathrm{nuc}} - \lambda_4 C_3^{\mathrm{nuc}} + \mu_5 R_2^{\mathrm{nuc}} C_1^{\mathrm{nuc}} - \lambda_5 C_3^{\mathrm{nuc}}
\end{aligned}
\tag{7}
$$

Abbreviations, parameters and chemical reaction equations are summarized in Table1,2 and 3.

Appendix B

Here we derive the analytical formula for the final concentration of homo-dimer, hetero-dimer, homo-trimer and hetero-trimer as a function of the ratio of initial concentration of R-Smad to Co-Smad monomers. Assuming $\mu = 0$ in Eq(6) and Eq(3) in the text, rescaling time, and letting $\lambda = \beta R/\alpha$ yields

$$\frac{dx_0}{dt} = -\lambda x_0 \tag{A1a}$$
$$\frac{dx_1}{dt} = \lambda x_0 - x_1(2x_1 + x_2 + y_1 + y_2) \tag{A1b}$$
$$\frac{dx_2}{dt} = x_1^2 - x_2(x_1 + y_1) \tag{A1c}$$
$$\frac{dx_3}{dt} = x_1 x_2 \tag{A1d}$$
$$\frac{dy_1}{dt} = -y_1(x_1 + x_2) \tag{A1e}$$
$$\frac{dy_2}{dt} = x_1 y_1 - y_2 x_1 \tag{A1f}$$
$$\frac{dy_3}{dt} = x_1 y_2 + x_2 y_1 \tag{A1g}$$

with the initial conditions: $x_0(0) = r/(1+r)$, $y_1(0) = 1/(1+r)$, $x_i(0) = 0$ $(i = 1, 2, 3)$, $y_i(0) = 0$ $(i = 2, 3)$.

Slow phosphorylation and $r < 2$

Assume that λ is small (slow phosphorylation), and that the initial Co-Smad monomers are more abundant than R-Smad (inactive) monomers. The active R-Smad monomers are only gradually supplied, which are then rapidly consumed by its binding to abundant Co-Smad monomers. We therefore expect that R-Smad monomers and home-dimers remain small. Let us rescale the time

in unit of the mean phosphorylation time as $T = \lambda t$, and let $x_1 = \lambda X_1$, $x_2 = \lambda X_2$ to have

$$\begin{aligned}
\frac{dx_0}{dT} &= -x_0 && \text{(A2a)}\\
\frac{dX_1}{dT} &= \frac{1}{\lambda}\left(x_0 - X_1(y_1+y_2)\right) - X_1(2X_1+X_2) && \text{(A2b)}\\
\frac{dX_2}{dT} &= X_1(X_1-X_2) - \frac{1}{\lambda}X_2 y_1 && \text{(A2c)}\\
\frac{dx_3}{dT} &= \lambda X_1 X_2 && \text{(A2d)}\\
\frac{dy_1}{dT} &= -y_1(X_1+X_2) && \text{(A2e)}\\
\frac{dy_2}{dT} &= X_1(y_1-y_2) && \text{(A2f)}\\
\frac{dy_3}{dT} &= (X_1 y_2 + X_2 y_1) && \text{(A2g)}
\end{aligned}$$

For $\lambda \to 0$ we see that $x_0 - X_1(y_1+y_2) \approx 0$ and $X_2 \approx 0$, $x_3 \approx 0$ to have the approximate system

$$\begin{aligned}
\frac{dx_0}{dT} &= -X_1(y_1+y_2) && \text{(A3a)}\\
\frac{dy_1}{dT} &= -y_1 X_1 && \text{(A3b)}\\
\frac{dy_2}{dT} &= X_1(y_1-y_2) && \text{(A3c)}\\
\frac{dy_3}{dT} &= X_1 y_2 && \text{(A3d)}
\end{aligned}$$

Introducing

$$\tau = \int_0^T X_1(s)ds,$$

we have a linear system

$$\begin{aligned}
\frac{dx_0}{d\tau} &= -(y_1+y_2) && \text{(A4a)}\\
\frac{dy_1}{d\tau} &= -y_1 && \text{(A4b)}\\
\frac{dy_2}{d\tau} &= y_1 - y_2 && \text{(A4c)}\\
\frac{dy_3}{d\tau} &= y_2 && \text{(A4d)}
\end{aligned}$$

with $x_0(0) = r/(1+r)$ and $y_1(0) = 1/(1+r)$.

Solving this linear equations

$$x_0(\tau) = \frac{1}{1+r}\left\{(\tau+2)e^{-\tau} - (2-r)\right\} \tag{A5a}$$

$$y_1(\tau) = \frac{1}{1+r}e^{-\tau} \tag{A5b}$$

$$y_2(\tau) = \frac{1}{1+r}\tau e^{-\tau} \tag{A5c}$$

$$y_3(\tau) = \frac{1}{1+r}\left\{1 - (1+\tau)e^{-\tau}\right\} \tag{A5d}$$

At the equilibrium x_0 must vanish and hence

$$(2-r) = (\tau_\infty + 2)e^{-\tau_\infty}. \tag{A6}$$

With τ_∞ defined above (which is well defined if $r < 2$), the equilibrium concentrations are expressed as

$$\hat{y}_1 = \frac{2-r}{1+r}\cdot\frac{1}{2+\tau_\infty}, \tag{A7a}$$

$$\hat{y}_2 = \frac{2-r}{1+r}\cdot\frac{\tau_\infty}{2+\tau_\infty}, \qquad (r<2), \tag{A7b}$$

$$\hat{y}_3 = \frac{1}{1+r}\cdot\frac{r+(r-1)\tau_\infty}{2+\tau_\infty}. \tag{A7c}$$

In this approximation, all R-Smads are converted either to RC or RRC. Indeed, using (A6) and (A7) we can show that

$$\hat{y}_2 + 2\hat{y}_3 = \frac{r}{1+r} = x_0(0). \tag{A8}$$

Slow phosphorylation and $r > 2$

Now we assume that initially R-Smads are more than twice as abundant as Co-Smads, keeping the assumption of small λ.

Co-Smad monomers are gradually but consistently consumed because active R-Smad monomers are consistently produced until all the Co-Smad monomers are used up. With the same reason all

the heterodimers (RC) are converted to heterotrimers. Thus the conservation of Co-Smads

$$y_1 + y_2 + y_3 = \frac{1}{1+r} \tag{A9}$$

applied at equilibrium then yields

$$\hat{y}_1 = \hat{y}_2 = 0, \tag{A10a}$$

$$\hat{y}_3 = \frac{1}{1+r}. \qquad (r > 2) \tag{A10b}$$

Slow supply of active R-Smad monomers also guarantees that nearly all the monomers are converted to trimers (Nakabayashi and Sasaki 2006). Hence at equilibrium $\hat{x}_0 = \hat{x}_1 = 0$ and $\hat{x}_2 \approx 0$. The conservation of R-Smads

$$x_0 + x_1 + 2x_2 + 3x_3 + y_2 + 2y_3 = \frac{r}{1+r} \tag{A11}$$

applied at equilibrium then yields

$$\hat{x}_0 = \hat{x}_1 = \hat{x}_2 = 0, \tag{A12a}$$

$$\hat{x}_3 = \frac{r-2}{3(1+r)}. \qquad (r > 2) \tag{A12b}$$

To summarize, the approximate equilibrium concentration of Smad complexes in the limit

of slow phosphorylation ($\lambda \to 0$) are given as a function of $r = x_0/y_0$ as $\hat{x}_0 = \hat{x}_1 = 0$ and

$$\hat{x}_2 = [RR] = 0, \tag{A13}$$

$$\hat{x}_3 = [RRR] = \begin{cases} 0, & (r < 2), \\ \dfrac{r-2}{3(1+r)}, & (r > 2), \end{cases} \tag{A14}$$

$$\hat{y}_1 = [C] = \begin{cases} \dfrac{2-r}{1+r} \cdot \dfrac{1}{2+\tau_\infty}, & (r < 2), \\ 0, & (r > 2), \end{cases} \tag{A15}$$

$$\hat{y}_2 = [RC] = \begin{cases} \dfrac{2-r}{1+r} \cdot \dfrac{\tau_\infty}{2+\tau_\infty}, & (r < 2), \\ 0, & (r > 2), \end{cases} \tag{A16}$$

$$\hat{y}_3 = [RRC] = \begin{cases} \dfrac{1}{1+r} \dfrac{r+(r-1)\tau_\infty}{2+\tau_\infty}, & (r < 2), \\ \dfrac{1}{1+r}, & (r > 2). \end{cases} \tag{A17}$$

Here τ_∞ is defined as the unique positive root of (A6) which exists for $r < 2$.

References

Byfield, S. D. & Roberts, A. B. (2004). Lateral signaling enhances TGF-β response complexity. *Trends Cell Biol,* **14** (3), 107–111.

Feng, X. H. & Derynck, R. (2005). Specificity and versatility in TGF-β signaling through Smads. *Annu Rev Cell Dev Biol,* **21**, 659–693.

Goumans, M. J., Valdimarsdottir, G., Itoh, S., Lebrin, F., Larsson, J., Mummery, C., Karlsson, S. & ten Dijke, P. (2003). Activin receptor-like kinase (ALK)1 is an antagonistic mediator of lateral TGFP/ALK5 signaling. *Mol Cell,* **12** (4), 817–828.

Goumans, M. J., Valdimarsdottir, G., Itoh, S., Rosendahl, A., Sideras, P. & ten Dijke, P. (2002). Balancing the activation state of the endothelium via two distinct TGF-β type I receptors. *EMBO J,* **21** (7), 1743–1753.

Green, J. (2002). Morphogen gradients, positional information, and *Xenopus*: Interplay of theory and experiment. *Dev Dyn,* **225** (4), 392–408.

Gurdon, J. B. & Bourillot, P. Y. (2001). Morphogen gradient interpretation. *Nature,* **413** (6858), 797–803.

Hill, C. S. (2001). TGF-β signalling pathways in early *Xenopus* development. *Curr Opin Genet Dev,* **11** (5), 533–540.

Inman, G. J. & Hill, C. S. (2002). Stoichiometry of active Smad-transcription factor complexes on DNA. *J Biol Chem,* **277** (52), 51008–51016.

Kawabata, M., Imamura, T., Inoue, H., Hanai, J. I., Nishihara, A., Hanyu, A., Takase, M., Ishidou, Y., Udagawa, Y., Oeda, E., Goto, D., Yagi, K., Kato, M. & Miyazono, K. (1999). Intracellular signaling of the tgf-β superfamily by smad proteins. In *Anticancer Molecules: Structure, Function, and Design* vol. 886, of *Ann N Y Acad Sci* pp. 73–82.

Kawabata, M., Inoue, H., Hanyu, A., Imamura, T. & Miyazono, K. (1998). Smad proteins exist as monomers in vivo and undergo homo- and hetero-oligomerization upon activation by serine/threonine kinase receptors. *EMBO J,* **17** (14), 4056–4065.

Massague, J., Seoane, J. & Wotton, D. (2005). Smad transcription factors. *Genes Dev,* **19** (23), 2783–2810.

Miyazono, K. (2000). Positive and negative regulation of TGF-β signaling. *J Cell Sci,* **113** (7), 1101–1109.

Moustakas, A. & Heldin, C. H. (2002). From mono- to oligo-Smads: The heart of the matter in TGF-β signal transduction. *Genes Dev,* **16** (15), 1867–1871.

Nakabayashi, J. & Sasaki, A. (2006). A mathematical model for apoptosome assembly: The optimal cytochrome c/Apaf-1 ratio. *J. Theol. Biol.* **242** (3), 280–287.

Podos, S. D. & Ferguson, E. L. (1999). Morphogen gradients - New insights from DPP. *Trends Genet,* **15** (10), 396–402.

Schmierer, B., Tournier, A. L., Bates, P. A. & Hill, C. S. (2008). Mathematical modeling identifies smad nucleocytoplasmic shuttling as a dynamic signal-interpreting system. *Proc Natl Acad Sci U S A,* **105** (18), 6608–13.

Shi, Y. G. & Massague, J. (2003). Mechanisms of TGF-β signaling from cell membrane to the nucleus. *Cell,* **113** (6), 685–700.

ten Dijke, P. & Hill, C. S. (2004). New insights into TGF-β-Smad signalling. *Trends Biochem Sci,* **29** (5), 265–273.

ten Dijke, P., Miyazono, K. & Heldin, C. H. (2000). Signaling inputs converge on nuclear effecters in TGF-β signaling. *Trends Biochem Sci,* **25** (2), 64–70.

Wu, J. W., Fairman, R., Penry, J. & Shi, Y. G. (2001). Formation of a stable heterodimer between Smad2 and Smad4. *J Biol Chem,* **276** (23), 20688–20694.

Yeo, C. Y., Chen, X. & Whitman, M. (1999). The role of FAST-1 and Smads in transcriptional regulation by activin during early *Xenopus* embryogenesis. *J Biol Chem,* **274** (37), 26584–26590.

actual name	name in the model	abbreviation	stoichiometry	one-way model
Smad-1 -2 -3 -5 -8	inactive R-Smad	R_0		x_0
	phosphorylated R-Smad	R_1	R	x_1
	homo-dimer	R_2	RR	x_2
	homo-trimer	R_3	RRR	x_3
Smad-4	Co-Smad	C_1	C	y_1
	hetero-dimer	C_2	RC	y_2
	hetero-trimer	C_3	RRC	y_3

Table 1: The stoichiometry of various Smad complexes

1	$\mathrm{TGF}\beta + R \xrightarrow{\alpha} R^*$	receptor activation
2	$R^* + R_0^{\mathrm{cyt}} \xrightarrow{\gamma} R_1$	phosphorylation
3	$R_0^{\mathrm{cyt}} \underset{Kr_{\mathrm{out}}}{\overset{Kr_{\mathrm{in}}}{\rightleftarrows}} R_0^{\mathrm{nuc}}$	shuttling
4	$R_1^{\mathrm{cyt}} \underset{Kr_{\mathrm{out}}}{\overset{Kr_{\mathrm{in}}}{\rightleftarrows}} R_1^{\mathrm{nuc}}$	shuttling
5	$C_1^{\mathrm{cyt}} \underset{Kr_{\mathrm{out}}}{\overset{Kr_{\mathrm{in}}}{\rightleftarrows}} C_1^{\mathrm{nuc}}$	shuttling
6	$R_1^{\mathrm{cyt}} + R_1^{\mathrm{cyt}} \underset{\lambda_1}{\overset{\mu_1}{\rightleftarrows}} R_2^{\mathrm{cyt}}$	complex formation in cytoplasm
7	$R_1^{\mathrm{cyt}} + R_2^{cyt} \underset{\lambda_2}{\overset{\mu_2}{\rightleftarrows}} R_3^{\mathrm{cyt}}$	complex formation in cytoplasm
8	$R_1^{\mathrm{cyt}} + C_1^{cyt} \underset{\lambda_3}{\overset{\mu_3}{\rightleftarrows}} C_2^{\mathrm{cyt}}$	complex formation in cytoplasm
9	$R_1^{\mathrm{cyt}} + C_2^{\mathrm{cyt}} \underset{\lambda_4}{\overset{\mu_4}{\rightleftarrows}} C_3^{\mathrm{cyt}}$	complex formation in cytoplasm
10	$R_2^{\mathrm{cyt}} + C_1^{\mathrm{cyt}} \underset{\lambda_5}{\overset{\mu_5}{\rightleftarrows}} C_3^{\mathrm{cyt}}$	complex formation in cytoplasm
11	$R_1^{\mathrm{nuc}} + R_1^{\mathrm{nuc}} \underset{\lambda_1}{\overset{\mu_1}{\rightleftarrows}} R_2^{\mathrm{nuc}}$	complex formation in nucleus
12	$R_1^{\mathrm{nuc}} + R_2^{\mathrm{nuc}} \underset{\lambda_2}{\overset{\mu_2}{\rightleftarrows}} R_3^{\mathrm{nuc}}$	complex formation in nucleus
13	$R_1^{\mathrm{nuc}} + C_1^{\mathrm{nuc}} \underset{\lambda_3}{\overset{\mu_3}{\rightleftarrows}} C_2^{\mathrm{nuc}}$	complex formation in nucleus
14	$R_1^{\mathrm{nuc}} + C_2^{\mathrm{nuc}} \underset{\lambda_4}{\overset{\mu_4}{\rightleftarrows}} C_3^{\mathrm{nuc}}$	complex formation in nucleus
15	$R_2^{\mathrm{nuc}} + C_1^{\mathrm{nuc}} \underset{\lambda_5}{\overset{\mu_5}{\rightleftarrows}} C_3^{\mathrm{nuc}}$	complex formation in nucleus
16	$R_2^{\mathrm{cyt}} \xrightarrow{Kr^*_{\mathrm{in}}} R_2^{\mathrm{nuc}}$	shuttling
17	$R_3^{\mathrm{cyt}} \xrightarrow{Kr^*_{\mathrm{in}}} R_3^{\mathrm{nuc}}$	shuttling
18	$C_2^{\mathrm{cyt}} \xrightarrow{Kc^*_{\mathrm{in}}} C_2^{\mathrm{nuc}}$	shuttling
19	$C_3^{\mathrm{cyt}} \xrightarrow{Kc^*_{\mathrm{in}}} C_3^{\mathrm{nuc}}$	shuttling
20	$R_1^{\mathrm{nuc}} \xrightarrow{\delta_p} R_0^{\mathrm{nuc}}$	dephosphorylation

Table 2: chemical reaction equation

abbreviations	value	units	reactions
Kr_{in}	0.0026	s^{-1}	import rate of R-Smad monomer
Kr_{out}	0.0056	s^{-1}	export rate of R-Smad monomer
Kc_{in}	0.0026	s^{-1}	import rate of Co-Smad monomer
Kc_{out}	0.0026	s^{-1}	export rate of Co-Smad monomer
Kr^*_{in}	$5.7 \times Kr_{in}$	s^{-1}	import rate of homomeric complex of Smad
Kc^*_{in}	$5.7 \times Kc_{in}$	s^{-1}	import rate of heteromeric complex of Smad
α	0.074	$nM^{-1}s^{-1}$	TGFβ-receptor association
γ	0.0004	nM^{-1} s^{-1}	phosphorylation
δ_r	0.00005	s^{-1}	active receptor degradation
δ_p	0.00657	s^{-1}	dephosphorylation
μ_1 μ_2 μ_3 μ_4 μ_5	0.0018	$nM^{-1}s^{-1}$	complex formation
λ_1 λ_2 λ_3 λ_4 λ_5	0.016	s^{-1}	complex dissociation
[TGF-β](0)	1.0	nM	initial concentration of TGF-β
[TβR](0)	1.0	nM	initial concentration of TGF-β receptor
$R_0^{\mathrm{cyt}}(0) + R_0^{\mathrm{nuc}}(0)$	89.1	nM	total concentration of R-Smad
$C_1^{\mathrm{cyt}}(0) + C_1^{\mathrm{nuc}}(0)$	101.6	nM	total concentration of Co-Smad

Table 3: parameter

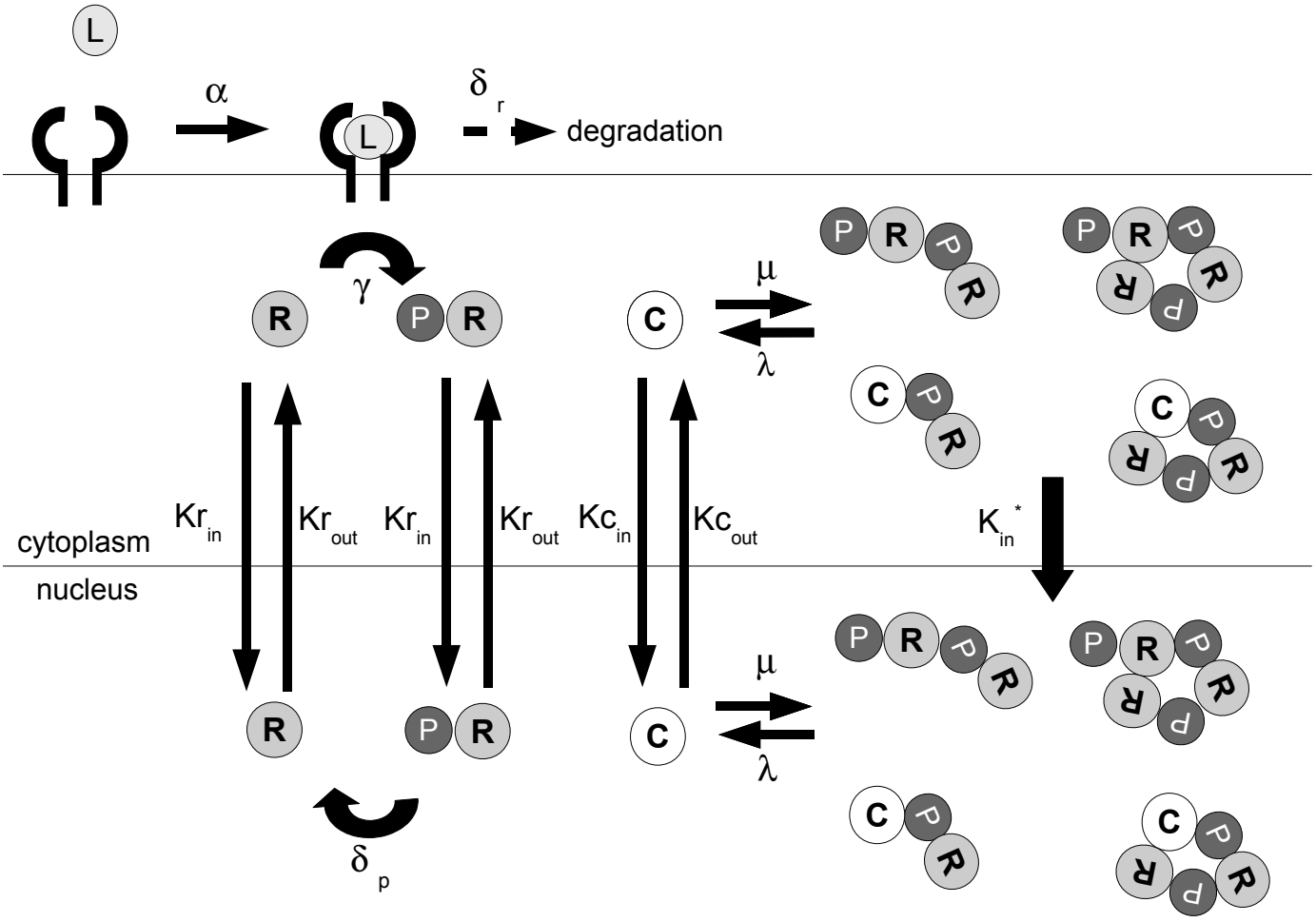

Figure 1: Schematic illustration of TGF-β signal transduction pathway. Type II TGF-β receptor binds TGF-β ligand forming heteromeric complex with type I receptor. Type I receptor recruit and phosphorylates receptor mediated Smad (R-Smad). Phosphorylated R-Smad can bind each other or common mediator Smad (Co-Smad). Smad monomers are reversibly imported and exported from cytoplasm and nucleus. On the other hands, Smad complexes irreversibly move into nucleus and regulate the transcriptional activity of the target genes. Phosphorylated R-Smad is dephosphorylated only in nucleus.

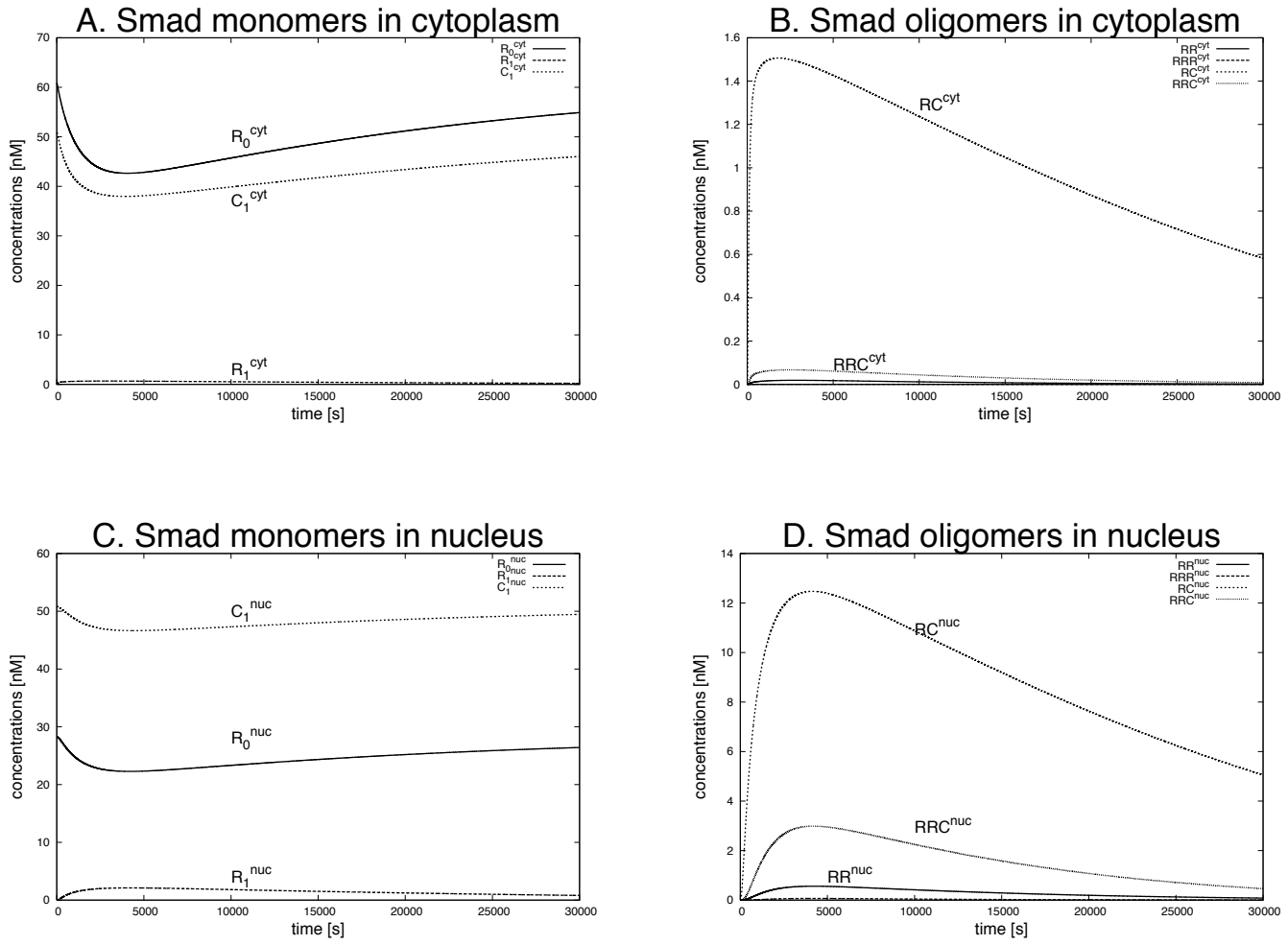

Figure 2: Time course of the Smad signal transduction obtained from two-compartment model(7). A: The concentrations of Smad monomers in cytoplasm are plotted. Smad is phosphorylated when the signal transduction started at time 0. After sufficiently long time for the degradation of the active receptor complex has passed, R_0^{cyt} and C_1^{cyt} are restored to the normal condition. B: The concentration of Smad oligomers in cytoplasm are plotted. The concentrations of Smad oligomers in cytoplasm are small because Smad oligomers is irreversibly transported to nucleus. C: The concentrations of Smad monomers in nucleus are plotted. Contrary to cytoplasm, the initial concentration of Co-Smad in nucleus is higher than that of R-Smad monomer in nucleus because export rate of Co-Smad is smaller than that of R-Smad. R_1^{nuc} is rapidly consumed by the oligomerization and is dephosphorylated in nucleus. D: The concentrations of Smad oligomers in nucleus are plotted. Hetero-dimer ($\mathrm{RC}^{\mathrm{nuc}}$) is predominantly accumulated in nucleus in response to the signal in this condition. The concentration of hetero-trimer ($\mathrm{RRC}^{\mathrm{nuc}}$ becomes higher than that of homo-dimer ($\mathrm{RR}^{\mathrm{nuc}}$) in nucleus. Homo-trimer is hardly accumulated in nucleus as well as in the cytoplasm. Parameters: $\alpha = 0.074[\mathrm{nM}^{-1}\mathrm{s}^{-1}]$, $\gamma = 0.0004[\mathrm{nM}^{-1}\mathrm{s}^{-1}]$, $\delta_r = 0.00005[\mathrm{s}^{-1}]$, $\delta_p = 0.00657[\mathrm{s}^{-1}]$, $\mu_1 = \mu_2 = \mu_3 = \mu_4 = \mu_5 = 0.0018[\mathrm{nM}^{-1}\mathrm{s}^{-1}]$, $\lambda_1 = \lambda_2 = \lambda_3 = \lambda_4 = \lambda_5 = 0.016[\mathrm{s}^{-1}]$, $Kr_{in} = 0.0026[\mathrm{s}^{-1}]$, $Kr_{out} = 0.0056[\mathrm{s}^{-1}]$, $Kc_{in} = 0.0026[\mathrm{s}^{-1}]$, $Kc_{out} = 0.0026[\mathrm{s}^{-1}]$. Initial conditions: [TGF-β] =1.0[nM], [TβR]=1.0[nM], total $R_0 = 89.1$[nM], total $C_1 = 101.6$[nM].

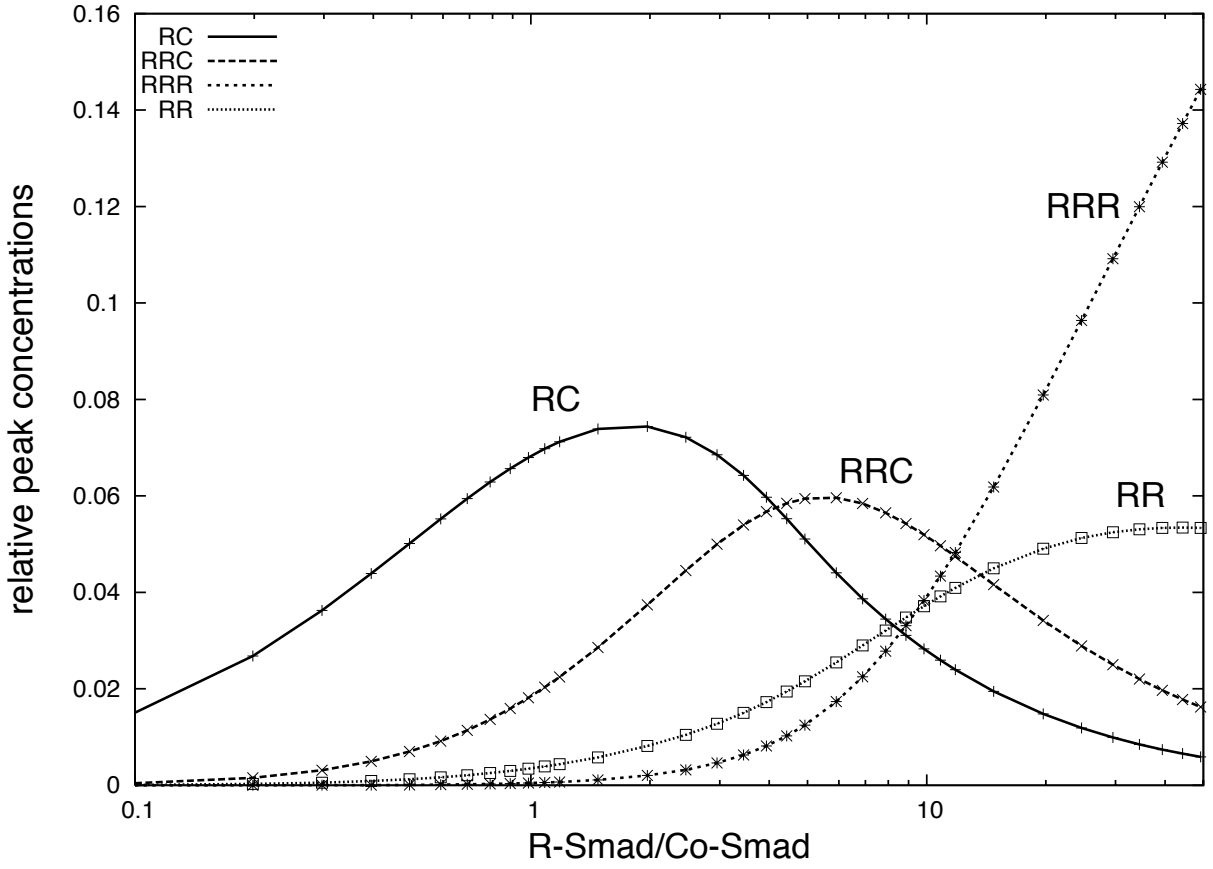

Figure 3: The relative peak concentrations of Smad oligomers to the initial Smad concentrations are plotted as a function of the initial R/C ratio. The initial concentration of Co-Smad is fixed as 101.6 [nM] and the concentration of R-Smad is varied from 10.16 [nM] to 5000.16 [nM]. Smad hetero-dimer (RC) are dominantly produced when R/C ratio is small or intermediate. As the R/C ratio increases, both hetero-trimer and homo-trimer are accumulated and homo-dimer are accumulated when R/C ratio is sufficiently large. The hetero-dimer is maximized around when R/C ratio is 2. On the other hand, hetero-trimer is maximized around R/C ratio is 5.

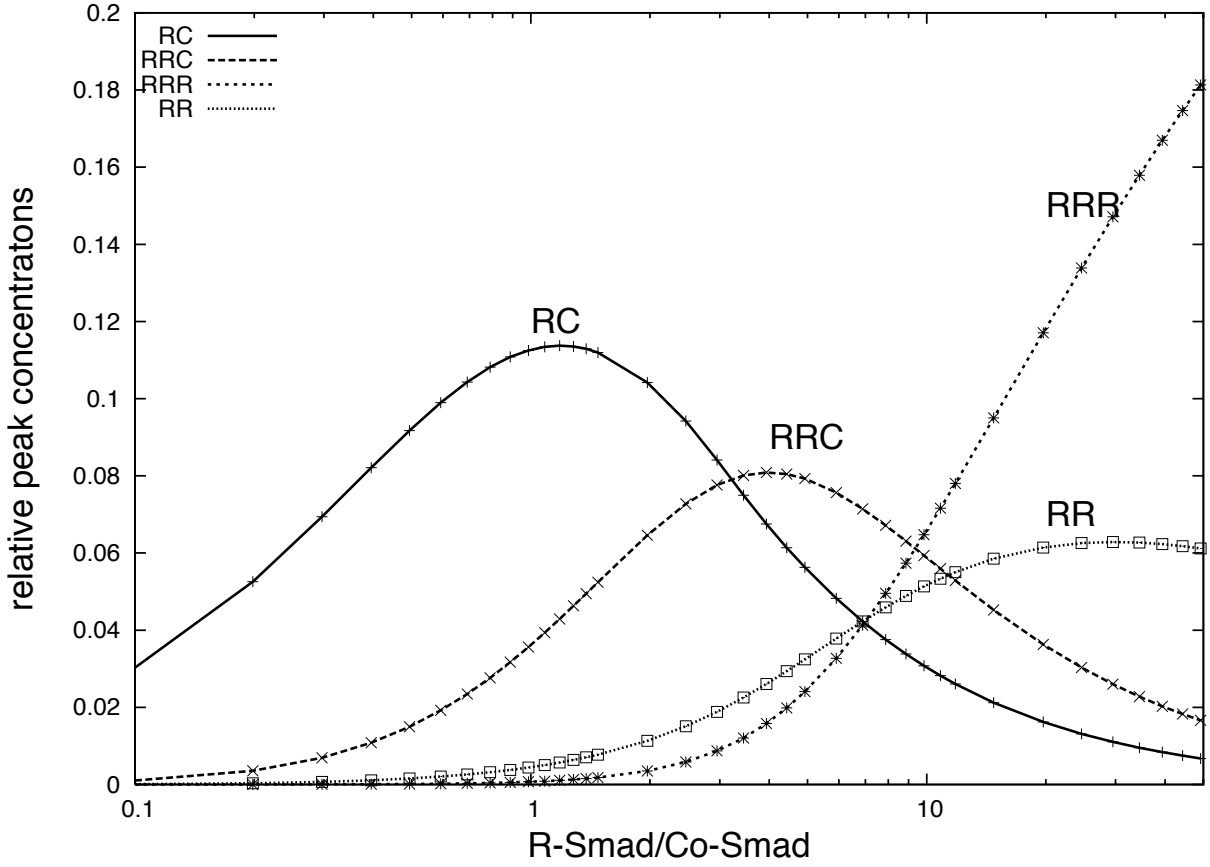

Figure 4: The relative peak concentrations obtained from single-compartment model (2). As well as shown in Fig 3, the relative peak concentration is plotted as a function of R/C ratio. The graph is slightly shifted to left as compare with Fig 4. The concentration of hetero-dimer is maximized when R/C ratio is 1 and hetero-trimer is maximized when R/C ratio is from 3 to 4.

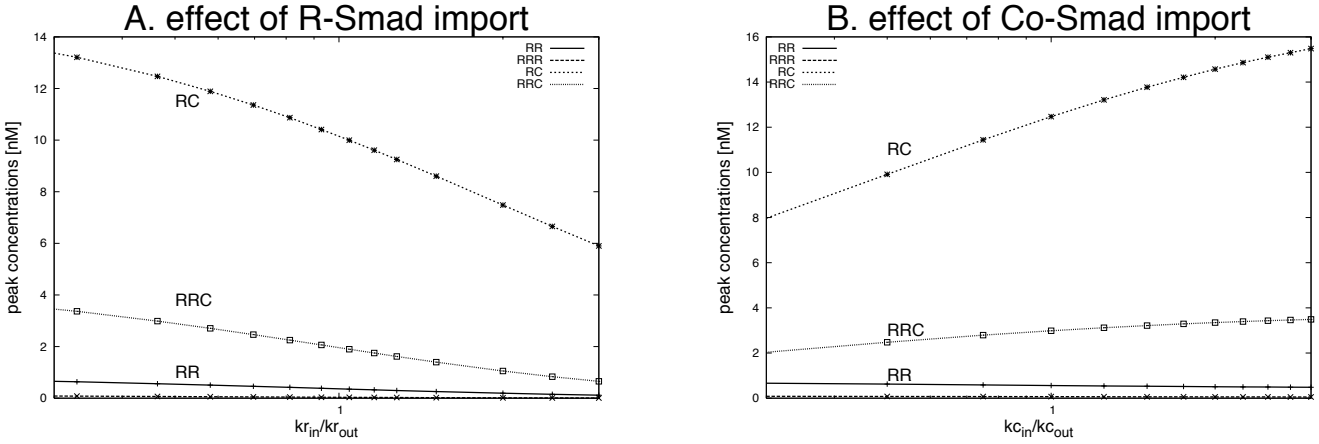

Figure 5: A: The effect of the import rate of R-Smad. The peak concentrations of all Smad oligomers monotonically decrease depending on the ratio of the import to the export rate constant of R-Smad. The accumulation of R-Smad in nucleus inhibits the phosphorylation of R-Smad. B: The effect of the import rate of Co-Smad. The peak concentration of heteromeric complex of Smad is specifically increased by increasing the import rate of Co-Smad. The predominant production of heteromeric complex of Smad is enhanced by the accumulation of Co-Smad to nucleus but not R-Smad.

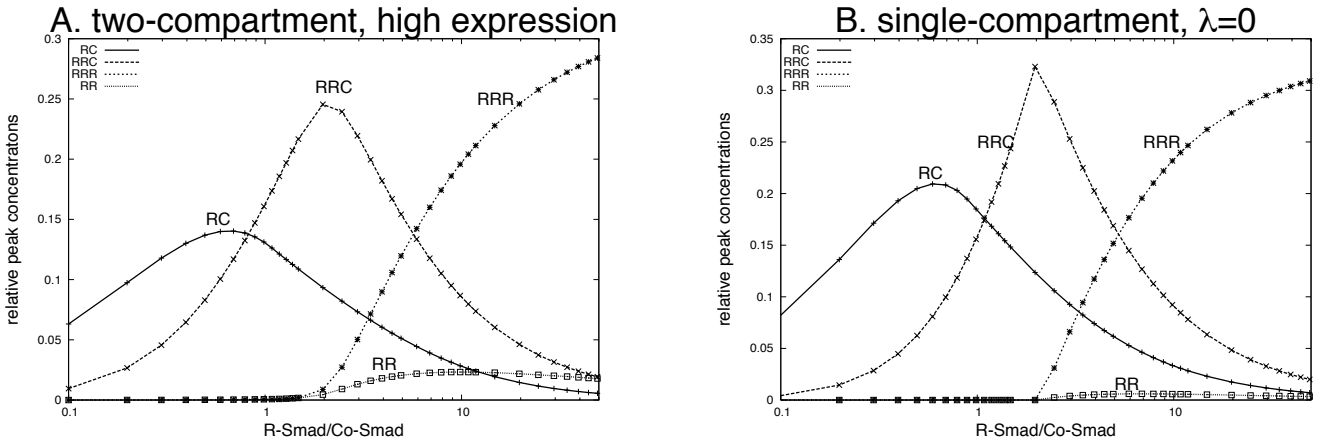

Figure 6: A: The relative peak concentration of Smad oligomers in two-compartment model when the expression level of R- and Co-Smad is large (100 times Co-Smad expression in Fig 4). The peak concentration of hetero-trimer increases as compared with Fig 3. Though the conversion efficiency is changed depending on the expression level of Smads, the relationship between R/C ratio and the predominant Smad species is qualitatively conserved. Hetero-dimer is predominantly produced when R/C ratio is small and intermediate. And then, hetero-trimer is maximized when R/C ratio becomes 2. The threshold R/C ratio switching both from homo-dimer to hetero-trimer and from hetero-trimer to homo-trimer becomes clear. The result obtained from two-compartment model becomes close to Fig 7 as Smad expression increases. B: The relative peak concentration of Smad oligomers in single-compartment model when $\lambda = 0$. As well as Fig 6-A, the relative peak concentration of hetero-trimer increases. The conversion efficiency of Smad complex formation from monomer to oligomers is improved by omitting the dissociation of Smad complex.

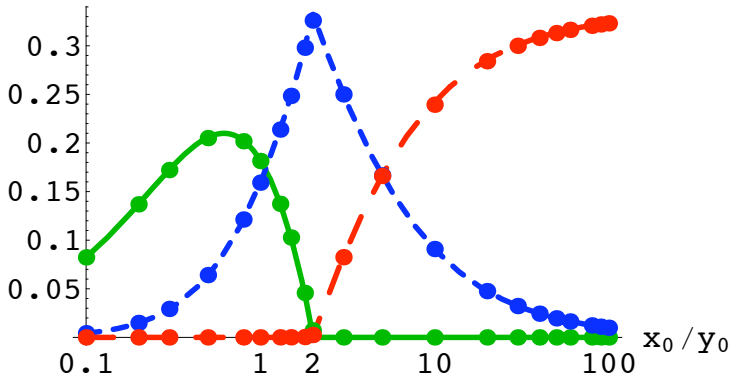

Figure 7: Analytical result which Smad species is predominantly produced. This graph show the case when R-Smad is slowly phosphorylated with small βR ($\beta R = 0.001$). Green solid, blue dashed and red small dashed line show the concentration of hetero-dimer, hetero-trimer and homo-trimer, respectively. Lines and dots indicate the analytical results obtained in Appendix and the numerical results, respectively. The concentration of Homo-dimer are almost 0 around the all region. This result well coincides with the results obtained from both two-compartment model with the large Smads expression in Fig 6-A and from single-compartment model without dissociation in Fig 6-B. The conversion efficiency from dimer to trimer is improved by the slow phosphorylation of R-Smad in the following sense (Nakabayashi & Sasaki, 2006). The slow phosphorylation decreases the final concentrations of homo- and hetero-dimer when the initial concentration of R-Smad is large, because it prolongs the period during which phosphorylated R-Smad monomer can contribute to form the homo- and the hetero-trimer.

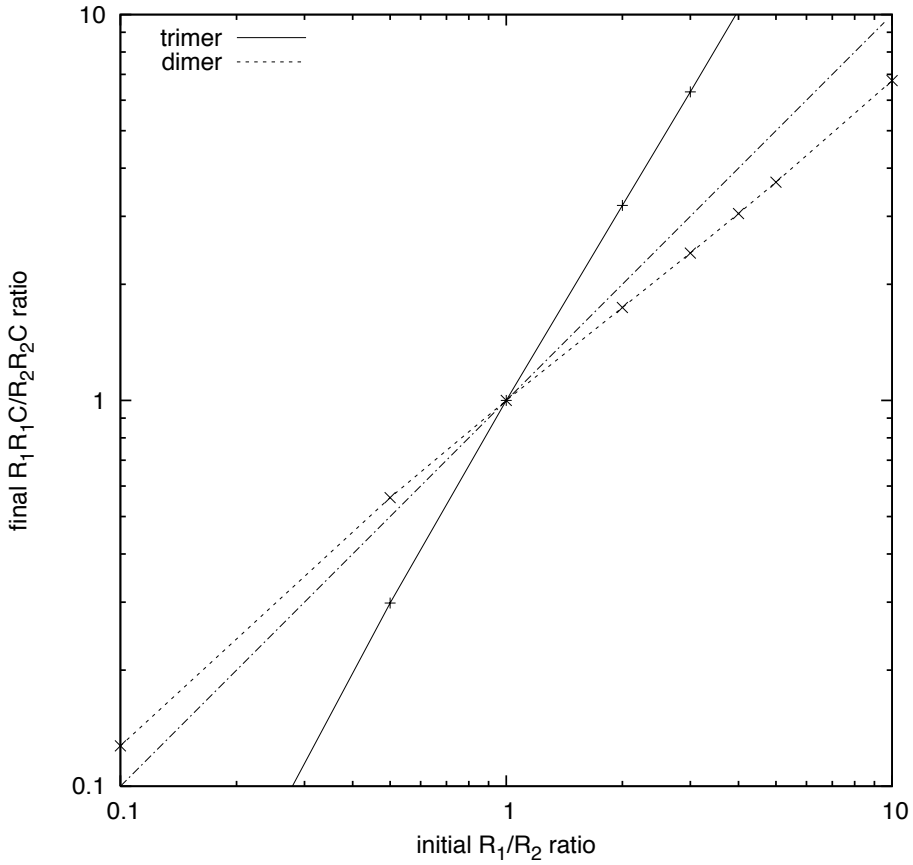

Figure 8: The ratio of the final product induced by the ALK-1 signal (R_1R_1C) to that induced by the ALK-2 signal (R_2R_2C) as a function of the initial ratio of the two signals (solid line). For comparison the corresponding quantity when the final product was dimer (R_1C to R_2C) rather than trimer is plotted as dashed line. The slope becomes larger than 1 (small dotted line) when the final product is trimer. In the right end of this graph, the initial 10 times ratio Smad-1/Smad-2 is enhanced about 50 times if the final product is trimer, but will be reduced to 5 times if it were dimer. This result indicates that more accurate switching in response to ligands is realized in ALK-1/ALK-2 signal transduction by the use of trimer rather than monomer or dimer.